Available online at www.sciencedirect.com
SCIENCE DIRECT
Biochimica et Biophysica Acta 1708 (2005) 154–163
BIOCHIMICA ET BIOPHYSICA ACTA
BBA
http://www.elsevier.com/locate/bba

Photosystem I lacking the PSI-G subunit has a higher affinity for plastocyanin and is sensitive to photodamage

Agnieszka Zygadlo[a], Poul Erik Jensen[a], Dario Leister[b], Henrik Vibe Scheller[a,*]

[a]*Plant Biochemistry Laboratory, Department of Plant Biology, The Royal Veterinary and Agricultural University, 40 Thorvaldsensvej, DK-1871 Frederiksberg C, Denmark*
[b]*Abteilung für Pflanzenzüchtung und Ertragsphysiologie, Max-Planck-Institut für Züchtungsforschung, Carl-von-Linné Weg 10, 50829 Köln, Germany*

Received 2 November 2004; received in revised form 9 February 2005; accepted 17 February 2005
Available online 3 March 2005

Abstract

PSI-G is an 11 kDa subunit of PSI in photosynthetic eukaryotes. *Arabidopsis thaliana* plants devoid of PSI-G have a decreased PSI content and an increased activity of $NADP^+$ photoreduction in vitro but otherwise no obvious phenotype [P.E. Jensen, L. Rosgaard, J. Knoetzel, H.V. Scheller, Photosystem I activity is increased in the absence of the PSI-G subunit. J. Biol. Chem. 277, (2002) 2798–2803.]. To investigate the biochemical basis for the increased activity, the kinetic parameters of the reaction between PSI and plastocyanin were determined. PSI-G clearly plays a role in the affinity for plastocyanin since the dissociation constant (K_D) is only 12 μM in the absence of PSI-G compared to 32 μM for the wild type. On the physiological level, plants devoid of PSI-G have a more reduced Q_A. This indicates that the decreased PSI content is due to unstable PSI rather than an adaptation to the increased activity. In agreement with this indication of decreased stability, plants devoid of PSI-G were found to be more photoinhibited both at low temperature and after high light treatment. The decreased PSI stability was confirmed in vitro by measuring PSI activity after illumination of a thylakoid suspension which clearly showed a faster decrease in PSI activity in the thylakoids lacking PSI-G. Light response of the P700 redox state in vivo showed that in the absence of PSI-G, P700 is more reduced at low light intensities. We conclude that PSI-G is involved in the binding dynamics of plastocyanin to PSI and that PSI-G is important for the stability of the PSI complex.

Keywords: Photosynthesis; Plastocyanin kinetic; Photosystem I; Photoinhibition

1. Introduction

PSI drives the light-mediated transfer of electrons from plastocyanin (Pc) on the luminal side of the thylakoid membrane to ferredoxin on the stromal side. PSI consists of at least 18 different subunits in higher plants including the four proteins belonging to the peripheral antenna (LHCI) [1]. The electron transfer components of PSI are the reaction center P700 (a chlorophyll *a* dimer), the primary acceptor A_0 (a chlorophyll *a* molecule), the secondary acceptor A_1 (a phylloquinone molecule), and the [4Fe–4S] iron–sulfur centers F_X, F_B and F_A [2,3]. The electron transfer components are all bound to the three essential subunits PSI-A, -B and -C. The heterodimer of PSI-A and PSI-B also binds the majority of the approximately 90 core chlorophyll molecules [4]. The photooxidized donor side of PSI reacts with reduced Pc in the lumen of the thylakoids. Oxidized Pc is reduced by the cytochrome b_6f complex and Pc thereby functions as a soluble and mobile electron carrier between cytochrome b_6f and PSI.

PSI-G is an 11 kDa subunit of PSI in eukaryotes, unique to higher plants and green algae. PSI-G has some sequence similarity (30% amino acid identity) to the PSI-K subunit, which is found in PSI in all organisms, including cyanobacteria. PSI-G and PSI-K do not form any cross-linking products with other core subunits of PSI except for PSI-A and PSI-B [5]. This suggested that PSI-G and PSI-K are located away from the two-fold symmetry axis. This location was confirmed for PSI-K in cyanobacteria [2].

* Corresponding author. Fax: +45 3528 3333.
E-mail address: hvs@kvl.dk (H.V. Scheller).

0005-2728/$ - see front matter © 2005 Elsevier B.V. All rights reserved.
doi:10.1016/j.bbabio.2005.02.003

Using antisense plants [6] and knock-out lines [7], it has been shown that PSI-K is involved in binding of the Lhca2 and Lhca3 subunits of LHCI. Recently, Ben-Shem et al. [4] published a PSI crystal structure from pea with a 4.4 Å resolution. The structural model confirms the location of PSI-G on the opposite side of the reaction center compared to PSI-K and in close vicinity to LHCI proteins. In spite of the close association between PSI-G and LHCI, the PSI-G protein is not needed for binding or function of LHCI [8]. In the absence of PSI-G the PSI complex appeared to lose some additional subunits, possibly LHCI, upon mild solubilization and electrophoresis in green gels. Plants in which the expression of PSI-G is suppressed by an antisense *psaG* gene have 40% less PSI on a chlorophyll basis than wild type plants [8]. On the other hand, PSI isolated from plants lacking PSI-G contained all other PSI subunits in a normal stoichiometric ratio [8]. Surprisingly, PSI devoid of the PSI-G subunit has about 40% higher activity based on in vitro $NADP^+$ photoreduction measurements [8]. According to the structural model of plant PSI, PSI-G is located away from all the electron carriers in PSI and apparently also away from the docking sites for Pc and ferredoxin. Therefore, it is very surprising that a peripheral subunit such as PSI-G can affect electron transport through PSI.

It can be assumed that the PSI-G subunit could modulate the electron transfer rate either from Pc to P700 or from the terminal iron–sulfur cluster (F_B) to ferredoxin. Two of the small PSI subunits are known to influence the docking of Pc to PSI: PSI-N [9] and PSI-F [10,11]. The three-dimensional structure of PSI does not reveal the docking sites for the mobile electron carriers Pc and ferredoxin, and PSI-N is not present in the structural model [4]. In order to address the function of PSI-G further we first analyzed the interaction between Pc and PSI. Under our standard conditions for determining $NADP^+$ photoreduction, the reaction is limited by Pc and therefore we found that this reaction was most likely to be affected in the mutant PSI. To further investigate the role of PSI-G, we also studied the sensitivity to photoinhibition and the stability of PSI in the absence of the PSI-G subunit both in vitro and in vivo.

2. Materials and methods

2.1. Plant material and growth conditions

Arabidopsis thaliana (L.) Heynh. ecotype Columbia was used for all experiments. Plants were grown in compost in a controlled environment Arabidopsis Chamber (Percival AR-60L, Boone, IA) at a photosynthetic flux of 100–120 μmol photons m^{-2} s^{-1}, 20 °C, and 70% relative humidity. The photoperiod was 8 h to suppress the induction of flowering. The production of plants lacking PSI-G by antisense suppression or transposon footprint has been described previously [7,8].

Photoinhibition at chilling conditions was carried out by transferring plants to 4 °C at the beginning of the photoperiod as previously described [12,13].

2.2. Isolation of thylakoid membranes

Leaves from 8–10 week-old plants were used for isolation of thylakoids as described previously [9]. Total chlorophyll and chlorophyll a/b ratio in thylakoids were determined in 80% acetone according to the method of Lichtenhaler [14].

2.3. Isolation of plastocyanin

The procedure for isolation of Pc was based on the method of Ellefson et al. [15]. Spinach leaves from a local market were homogenized in 50 mM Tris (pH 8.0), 50 mM NaCl, 0.2 M sucrose, 5 mM $MgCl_2$ and filtered through two layers of nylon mesh. After centrifugation (12,000 ×g, 30 min) the pellet was resuspended in 0.5 M Tris (pH 8.0), ice cold acetone was added to 35% (v/v) final concentration, and the preparation was stirred for 10 min. After centrifugation (15,000 ×g, 10 min), cold acetone was added to the supernatant to 80% (v/v) final concentration, and the preparation was stirred for 30 min. After centrifugation (2500 ×g, 15 min), the pellet was air dried and resuspended in 50 mM potassium phosphate (pH 7.6). Bio-Rad AGI-X8 resin was added (0.5 g per 100 ml) and the sample was dialyzed over night in 6000 kDa cut-off dialysis tubing against 20 mM potassium phosphate (pH 7.6). After centrifugation (10,000 ×g, 10 min), the supernatant was loaded on a DEAE–Sepharose column (40 × 2.6 cm) equilibrated in 20 mM potassium phosphate (pH 7.6). The column was eluted with a linear gradient from 50 to 800 mM NaCl in 20 mM potassium phosphate (pH 7.6). Fractions containing Pc were identified by blue color after the addition of potassium ferricyanide. The combined fractions were precipitated with 55% saturated ammonium sulfate for 20 min at 4 °C. After centrifugation (12,000 ×g, 10 min), the Pc containing supernatant was dialyzed against 20 mM potassium phosphate (pH 7.6). The dialyzed product was concentrated by ultrafiltration and was loaded onto a Sephadex G50 superfine column (100 × 1.6 cm), equilibrated in 50 mM potassium phosphate (pH 7.6). Eluted fractions were analyzed by SDS-PAGE and Coomassie Blue staining. Fractions containing only pure Pc were frozen and stored at −80 °C. The concentration of Pc was determined from the ferricyanide-oxidized minus ascorbate-reduced difference spectrum using an extinction coefficient of 4.9 mM^{-1} cm^{-1}.

2.4. Kinetic measurements

Flash-induced P700 absorption decay was measured at 834 nm, as described previously [16,17]. The saturating actinic pulse (532 nm, 6 ns) was produced by a Nd:YAG

laser. Thylakoids (20 μg of chlorophyll) were dissolved in a final volume of 300 μl of 20 mM Tricine (pH 7.5), 40 mM NaCl, 8 mM $MgCl_2$, 0.1% digitonin, 2 mM sodium ascorbate, 6 μM 2,6-dichlorophenolindophenol and 100 μM methylviologen. The solution was incubated on ice in darkness for 10 min and centrifuged once for 10 s at 200 $\times g$ to remove starch. The sample (300 μl) was transferred to a cuvette with 1 cm path length and Pc was added to the required concentration, from 5 to 500 μM. A diode laser provided the measuring beam, which was detected using a photodiode. The signal was passed via a preamplifier (Tektronix ADA400A) to an oscilloscope. The time resolution with this setup is about 2.5 μs. A total of 32 absorbance transients were collected with 4 s interval and averaged for each decay curve. The recorded absorbance changes were resolved into three exponential decay components using a Levenberg–Marquardt non-linear regression procedure. Kinetic parameters were calculated from the exponential decays essentially according to Drepper et al. [17]. For details see the Results section.

2.5. Immunoblotting

Thylakoids were used for immunoblotting, which was carried out as previously described [6]. Secondary antibodies were detected using a chemiluminescence detection system (ECL, Amersham Biosciences).

2.6. Fluorescence measurements

Determination of conventional fluorescence parameters was performed with a PAM 101-103 fluorometer (Walz, Effeltrich, Germany) using a standard setup [9]. Photochemical quenching ($q_P=(F'_m-F_s)/(F'_m-F'_0)$) was determined in WT and ΔPSI-G leaves in the growth chamber (120 μmol photons m^{-2} s^{-1}). For the PSII photoinhibition measurements, the maximum quantum yield of PSII was determined as $Fv/Fm=(F_m-F_0)/F_m$ in leaves that were dark-adapted for 20 min prior to the measurement.

2.7. P700 oxidation state in WT and ΔPSI-G leaves

The redox level was monitored at 810 and 860 nm with a PAM 101–103 chlorophyll fluorometer (Walz, Effeltrich, Germany) connected to a dual wavelength emitter–detector unit ED 700 DW as described by Klughammer and Schreiber [18]. The dual wavelength emitter–detector system detects strictly differential absorbance changes (810 minus 860 nm) and is selective for absorbance changes caused by P700 [19]. Oxidized P700 (ΔAmax) was recorded during far-red light illumination. The level of oxidized P700 in the leaf (ΔA) was determined during white light illumination (from 25 to 800 μmol photons m^{-2} s^{-1}). PSI acceptor side limitation was determined using 50 ms flashes from a Walz XST 103 unit. Flashes were applied during the actinic light (SF_{al}) and the far-red (SF_{fr}) illuminations and the acceptor side limitation calculated as $(SF_{fr}-SF_{al})/SF_{fr}$.

2.8. Stability of PSI in isolated thylakoids and $NADP^+$ photoreduction measurements

Thylakoid suspension (50 μg chlorophyll per ml in a buffer of 20 mM Tricine (pH 7.5), 10 mM NaCl, 5 mM $MgCl_2$) was illuminated with actinic light (150 μmol photons m^{-2} s^{-1}) in a 3 ml acrylic chamber thermostated at 20 °C. The suspension was gently stirred and 300 μl of the thylakoid suspension was removed every 30 min for determination of $NADP^+$ photoreduction activity as described by Naver et al. [16] using thylakoids equivalent to 5 μg of chlorophyll. Thylakoids were solubilized in 0.1% *n*-dodecyl-β-D-maltopyranoside before measurement and saturating red light was used to drive the reaction.

3. Results

3.1. Binding dynamics and electron transfer between plastocyanin and PSI

Since the higher $NADP^+$ photoreduction activity of PSI from plants devoid of PSI-G suggests that PSI-G could have a role in the regulation of the reaction between P700 and Pc we decided to determine the kinetic parameters of this reaction. The reaction between Pc and P700 is a multi-step reaction, which can be divided into three major steps: binding of Pc to P700, electron transfer within a complex between Pc and P700, and release of oxidized Pc from the complex between Pc and P700 (Fig. 1A). To investigate the kinetics of the Pc–PSI interaction, flash-induced P700 absorption transients were determined in the presence of varying concentrations of Pc ranging from 0 to 500 μM. Flash excitation of PSI results in a very rapid absorption increase at 834 nm due to photo-oxidation of P700, followed by a slower absorption decrease due to reduction of $P700^+$ by Pc (Fig. 1B–D). Previous studies have demonstrated the possibility of monitoring the interaction between Pc and PSI by following the absorption at 820–835 nm [20–22]. The P700 absorption decrease can be modelled as the sum of three exponential decays discerned as a fast phase, an intermediate phase and a slow phase [20–22]. Each exponential decay component fitted to the obtained trace is characterized by two parameters: the amplitude A and a time constant τ. A fast phase (τ_1~10 μs) is due to intra-complex electron transfer from Pc bound to PSI prior to the flash [17,21,22]. The time constant τ_1 is independent of Pc concentration whereas the amplitude A_1 increases with increasing [Pc] (Fig. 2A). An intermediate phase (A_2) has a concentration-dependent time constant τ_2 and is related to the second-order reaction between unbound Pc and $P700^+$.

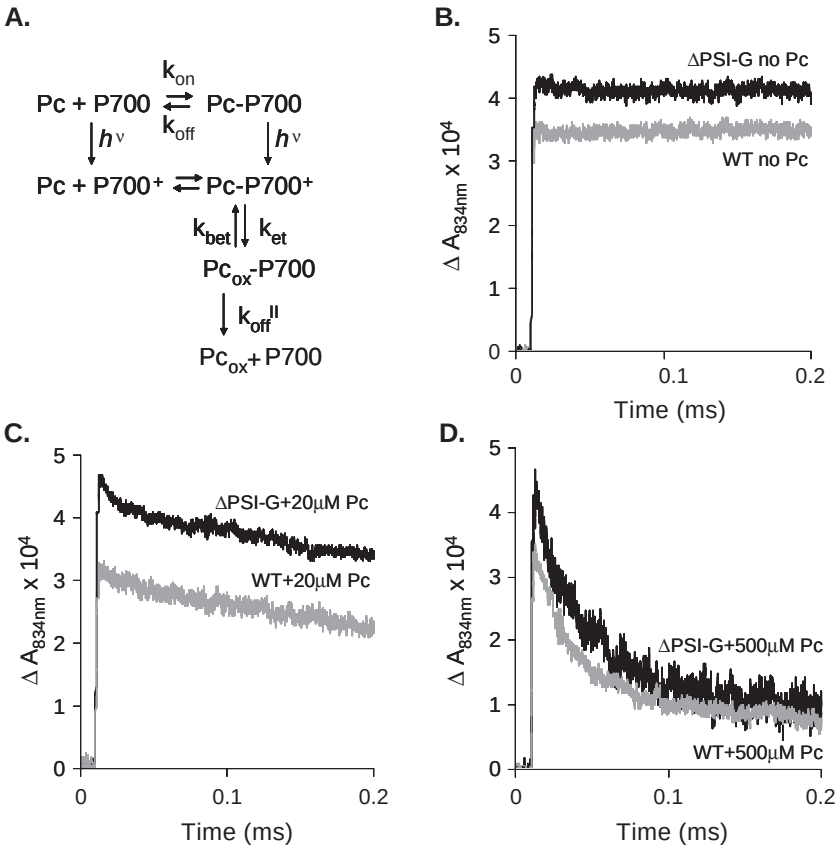

Fig. 1. Reaction between P700 and Pc in WT and ΔPSI-G plants. (A) Schematic model of the reaction between P700 and Pc. (B–D) Reduction of $P700^+$ by Pc in a 0.2 ms time scale. Flash-induced absorption changes were monitored at 834 nm in samples of solubilized thylakoids from WT and ΔPSI-G plants in the presence of 0 μM (B), 20 μM (C), 500 μM (D) of Pc. The traces shown are averages of 32 flashes spaced 4 s apart. The amplitude of PSI signal obtained from samples lacking PSI-G has been increased by multiplication with a factor of 1.3 to distinguish it clearly from the WT signal. Similar recordings were obtained at least nine times with each of the thylakoid preparations.

Finally, a slowly decaying absorption (A_3) is mostly due to absorption changes of Pc itself at 834 nm and is not seen if measurements are made at 700 nm [17,22]. As expected our data could be modelled as the sum of three exponential decays whereas two exponential decays gave a very poor fit and more than three decays did not significantly improve the fit. τ_1 was determined to 10 μs for both WT and ΔPSI-G at the highest concentrations of Pc. Since accurate estimation of τ_1 is difficult at low [Pc], its value was fixed to 10 μs to get a better estimation of the other parameters. Fig. 1C shows measurements with 20 μM as an example. Under these conditions, the fast absorption decrease (A_1) was larger in thylakoids devoid of PSI-G compared to WT thylakoids. The concentration of 20 μM is close to the dissociation constant (K_D) between Pc and P700 in WT plants (Table 1). From the extensive analysis with varying concentrations of Pc most of the rate constants of the reaction between Pc and P700 were estimated. Fig. 2 shows examples of the plots used to calculate the kinetic constants and the mean values obtained from several independent data sets are summarized in Table 1. The relative amplitude $A_1/(A_2+A_1)$ indicates the fraction of PSI participating in the electron transfer between Pc and P700 in a preformed complex (fast component A_1). At high Pc concentration (>80 μM) this fraction reaches a plateau at about 35% of the total oxidized P700 (Fig. 2A). The plot showing [Pc] divided by the relative amplitude $A_1/(A_2+A_1)$ as a function of [Pc] (Fig. 2B) can be used to calculate the dissociation constant K_D for Pc in the reduced form [17]. K_D is the intercept of the linear regression line with the abscissa and was found to be significantly higher (*t*-test, $p=0.001$) in WT PSI ($K_D=32$ μM) than in ΔPSI-G PSI ($K_D=12$ μM) (Fig. 2B), indicating that the affinity of P700 for Pc is higher in the absence of PSI-G. K_D is equal to the ratio k_{off}/k_{on}. The k_{on} constant can be estimated as the observed rate constant for the intermediate reaction $(1/\tau_2)$ at low [Pc] (Fig. 2C). No difference was found in k_{on} ($k_{on}=8\times10^7$ M^{-1} s^{-1}, Table 1) between WT and ΔPSI-G. Hence, the difference in K_D must be due to a difference in the k_{off} rate for reduced Pc. At high [Pc] essentially all PSI has Pc bound and available for intracomplex electron transfer. However, the limiting value for τ_2 is much longer (~50 μs) than τ_1 (=10 μs). This is because there is an equilibrium between Pc_{red}–$P700^+$ and Pc_{ox}–P700 and the observed decay is essentially limited by the dissociation of oxidized Pc from the complex [17]. Hence, the k_{off}^{II} rate for oxidized Pc can be estimated from the limiting value of t_2 at high [Pc] (Fig. 2D). At high concentration of Pc, the halftime approaches a

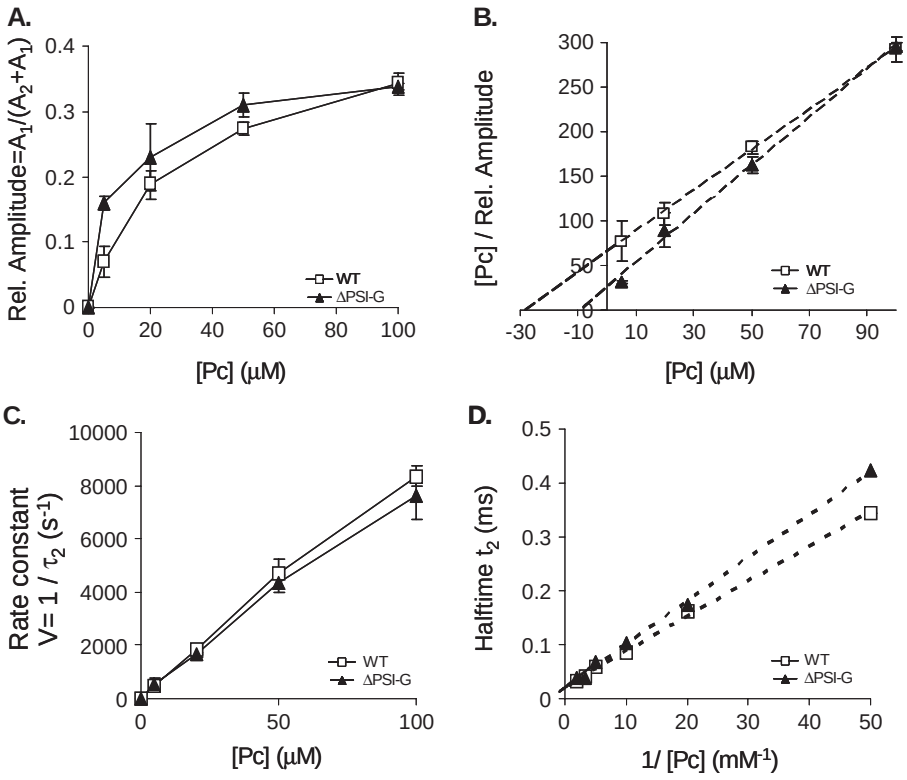

Fig. 2. Evaluation of the kinetic parameters in the reaction between Pc and P700. (A) Relative amplitude of the fast kinetic phase of $P700^+$ reduction $A_1/(A_2+A_1)$ as a function of Pc concentration. (B) Amplitude of the fast kinetic phase of $P700^+$ reduction $A_1/(A_2+A_1)$ as a function of plastocyanin concentration in a reciprocal plot. The intercept of the linear regression line with the abscissa is the dissociation constant (K_D). (C) Rate constant of the intermediate kinetic component as a function of the Pc concentration. The k_{on} constant is the coefficient of the trendline at low Pc concentration. (D) Reciprocal pseudo-first-order rate of the intermediate component as a function of the reciprocal value of the Pc concentration. The intercept of the linear regression lines with the ordinate axis represent the k_{off}^{II} constants. Two thylakoid preparations from knock-out PSI-G plants, one thylakoid preparation from antisense PSI-G plants and three thylakoid preparations from WT *Arabidopsis* plants were used. The values shown are averages ± SD of fitted curves of three measurements. Independent estimates of all parameters were obtained from similar curves obtained for each thylakoid preparation and used to calculate the values in Table 1.

saturating value around 35 μs and no significant difference was found between WT and ΔPSI-G. At high Pc concentration the fast phase of $P700^+$ reduction saturates at less than full signal, i.e. the intermediate phase does not disappear (Fig. 2A). This also reflects the equilibrium between Pc_{red}–$P700^+$ and Pc_{ox}–P700 determined by k_{et} (~1/τ_1) and k_{bet} [17]. We have estimated k_{et}/k_{bet} based on the $A_1/(A_2+A_1)$ ratio at very high Pc concentration (Figs. 1D, 2A) and find a value of 0.7 for both WT and ΔPSI-G.

Table 1
Kinetic parameters for binding dynamics and electron transfer between Pc and P700 in WT and ΔPSI-G plants

	Wild type	Δ PSI-G
K_D (μM)	31.5 ± 3.6	11. 6 ± 2.3
k_{on} (10^7 $M^{-1}s^{-1}$)	8.0 ± 0.6	8.0 ± 0.6
k_{et} (s^{-1})	10^5	10^5
k_{off}^{II} (10^4 s^{-1})	5.2 ± 1.4	4.6 ± 1.4

The constants of the reaction (Fig. 1A) were obtained from a curve-fitting analysis of data as shown in Fig. 1B,C,D with varying concentration of Pc. Three thylakoid preparations from plants lacking PSI-G (two preparations from knock-out plants and one from antisense plants), and three thylakoid preparations from WT *Arabidopsis* plants were used. At least three separate data sets were obtained with each thylakoid preparation and in each data set all measurements were done in triplicate. The values represent average ± SD (n=3) for all obtained data, where SD expresses the standard deviation between preparations.

In order to validate our measurements and compare with previous and very elaborate studies done with material from spinach [17], we also performed P700 decay measurements on spinach PSI. The estimated kinetic constants K_D and K_{off}^{II} of the reaction between P700 and Pc in spinach are in good agreement with Drepper et al. [17] (data not shown). The estimated value of only 0.7 for k_{et}/k_{bet} was also found in spinach as opposed to a much higher value in the study of Drepper et al. [17]. However, our method of estimating this value is less accurate and we do not want to emphasize this point.

In order to estimate how the determined differences in kinetic constants for the *Arabidopsis* samples would affect steady state electron transport, we simulated the production of Pc_{ox} as a function of time, using the reaction scheme in Fig. 1A and a step time of 1 μs. With a concentration of reduced Pc of 2 μM, which is the concentration normally used in our $NADP^+$ photoreduction assays, we could calculate a turnover rate of 129 s^{-1} $P700^{-1}$ and 142 s^{-1} $P700^{-1}$ for WT and ΔPSI-G, respectively. Thus, based on

the parameters deduced from the kinetic analysis, PSI without PSI-G would be predicted to have a higher turnover rate than WT PSI. This difference appears to account for some but not all the difference of 40% in steady state rate of $NADP^+$ photoreduction. It should be noted that a possible inaccuracy in the k_{et}/k_{bet} ratio does not affect the calculated turnover rates at low Pc concentration to a large extent. Calculated turnover rates are affected by k_{off}^{II} but at low Pc concentration the WT and mutant PSI are still significantly different when the standard deviations of k_{off}^{II} are taken into account. The concentration of Pc in the thylakoid lumen is two magnitudes higher than 2 μM [23]. However, the turnover observed in vitro or calculated by simulation with 2 μM Pc is around 100 s^{-1} which is very close to the turnover of 120–130 s^{-1} that can be calculated from in vivo rates of oxygen evolution under saturating light and CO_2 [9]. This indicates that the Pc pool is mostly oxidized under steady state illumination. Furthermore, we have determined in vitro $NADP^+$ reduction with up to 30 μM Pc and in all cases did the PSI without PSI-G show the same relative increase in activity compared to the WT (data not shown).

We conclude that PSI-G is directly or indirectly involved in the interaction between PSI and Pc and that in the absence of PSI-G, Pc has a three-fold higher affinity for binding to PSI. This difference in affinity is in agreement with a higher steady state rate of in vitro $NADP^+$ photoreduction as observed before [8].

3.2. Redox state of the plastoquinone pool

Having established that the primary cause for at least some of the increase in PSI activity in the absence of PSI-G is due to the interaction between PSI and Pc, it was of interest to analyze redox conditions in plants without PSI-G. These plants contain only approximately 60% PSI compared to the WT and the question was whether the lower content of PSI was an adaptation to the higher PSI activity or an indication of lower PSI stability. Plants with lower PSI activity respond with an increased PSI/PSII ratio which partially restores the redox balance [9,11]. If the lower PSI/PSII ratio in ΔPSI-G plants reflected a similar response to an increased PSI activity we would predict that the inter-system electron transport chain should be slightly more oxidized than in the WT.

Photochemical quenching is often used as an indicator for the redox level of the primary electron acceptor Q_A and therefore $1-q_P$ was measured directly in the growth chamber under the light conditions to which the plants were adapted. Under these conditions $1-q_P$ was almost three times higher in plants lacking PSI-G than in WT plants (Fig. 3). The difference is highly significant (*t*-test, $p<0.01$) indicating that even under these constant and optimal growth conditions the flow of electrons through the two photosystems is unbalanced in the absence of PSI-G and restricted by PSI. This result suggests that the lower PSI/PSII ratio is not an adaptation to the increased PSI activity but is an independent consequence of the lack of PSI-G. Plants devoid of PSI-G and consequently containing only approximately 60% PSI cannot fully compensate the electron flow by the increased activity of PSI. This suggests that PSI is less stable in the absence of the PSI-G subunit.

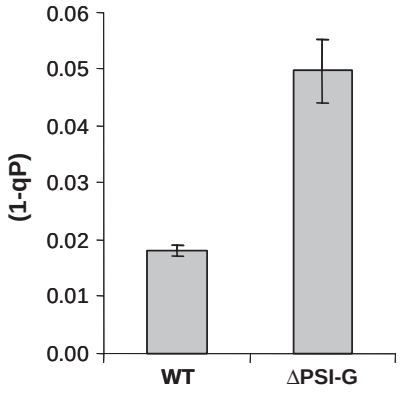

Fig. 3. Redox state of PSII acceptors. The reduction state of Q_A $(1-q_p)$ was estimated by measuring chlorophyll fluorescence in leaves from WT and ΔPSI-G plants in growth light (120 μmol photons m^{-2} s^{-1}). Shown is the average ± SE of measurement on five WT and six knock-out PSI-G plants.

3.3. Sensitivity to photoinhibition

In order to analyze if the absence of PSI-G plays a role in stability and sensitivity to photoinhibition, plants without PSI-G were subjected to different photoinhibitory conditions. Predominant PSI photodamage can be induced by exposing the plants to low temperature under moderate light [12], whereas predominant PSII photodamage is induced by high light [24,25].

In order to induce PSI photoinhibition WT plants and plants devoid of PSI-G were exposed to 4 °C for 8 h in growth light conditions (150 μmol photons m^{-2} s^{-1}) and subsequently PSII and PSI photochemistry were measured as photochemical efficiency (Fv/Fm) and $NADP^+$ photoreduction activity, respectively. After this treatment, plants devoid of PSI-G exhibited only a slightly higher sensitivity to PSII photoinhibition as Fv/Fm decreased about 10.4% in ΔPSI-G plants and 8.9% in WT plants (Table 2). However, PSI photochemistry was significantly more affected by the light treatment at low temperature. The WT plants showed a 10.2% decrease in PSI activity but the plants devoid of PSI-G were much more affected with a 22.8% decrease in PSI activity ($p=0.01$, two factor ANOVA) (Table 2).

Specific PSII photoinhibition was also induced by subjecting the plants to high light conditions (800 μmol photons m^{-2} s^{-1} at 20 °C for 3 h). Again Fv/Fm decreased only slightly more in the plants devoid of PSI-G (9%) than in WT plants (6.5%) (data not shown). Thus, PSII photoinhibition was almost the same in WT plants and plants devoid of PSI-G both under high light and chilling temper-

Table 2
Photoinhibition of WT and ΔPSI-G at chilling temperature

	Fv/Fm		PSI activity μmol NADPH s^{-1} μmol $P700^{-1}$	
	WT	ΔPSI-G	WT	ΔPSI-G
Dark 4 °C	0.807 ± 0.003	0.794 ± 0.008	38.3 ± 1.5	55.2 ± 3.4
Light 4 °C	0.735 ± 0.004	0.711 ± 0.002	34.4 ± 2.1	42.6 ± 1.9
% decrease	8.9 ± 0.6	10.4 ± 0.9	10.2 ± 0.7	22.8 ± 5.9

WT and knock-out from PSI-G plants were grown at 120 μmol photons m^{-2} s^{-1} and transferred from 20 to 4 °C. After 8 h, the leaves were harvested and thylakoids prepared for determination of PSI activity. Maximum PSII photochemical efficiency $Fv/Fm=(F_m-F_o)/F_m$ was determined directly on the intact leaves after 20 min of dark-adaptation. The values represent average ± SD ($n=4$). For both PSII and PSI the decrease was significantly higher in ΔPSI-G plants than in WT plants ($p=0.01$, two-factor ANOVA).

ature conditions. In contrast, plants lacking PSI-G were much more susceptible than the WT to photodamage of PSI.

3.4. Redox state of P700 in the leaf

In order to monitor the photosynthetic electron flow through PSI during steady state photosynthesis in vivo, we estimated the redox state of P700 in the light by measuring oxidation of P700 within the leaf as absorbance changes at 810 minus 860 nm. P700 was oxidized to $P700^+$ at different intensities of actinic light (ΔA) then reduced in the dark and finally oxidized to a maximum level of $P700^+$ under far-red illumination to favor PSI photochemistry (ΔA_{max}) (Fig. 4A). The light dependence of the P700 oxidation ratio ($\Delta A/\Delta A_{max}$) was examined in WT and ΔPSI-G plants. The redox state of P700 was identical at light intensities above 100 μmol $m^{-2}s^{-1}$ in WT and ΔPSI-G plants (Fig. 4B). However, at low light intensities (<100 μmol m^{-2} s^{-1}), the oxidation ratio of P700 was significantly lower in ΔPSI-G plants (Fig. 4B), indicating that P700 is more reduced in the absence of PSI-G.

The acceptor side limitation of PSI could also be estimated under different light intensities. A xenon flash was applied during actinic light illumination (SF_{al}) and during far-red light illumination (SF_{fr}) (Fig. 4A). The difference between the two flashes $(SF_{fr}-SF_{al})/SF_{fr}$ reflects the acceptor side limitation of PSI (Fig. 4C). The acceptor side of PSI in the absence of PSI-G was more limited (reduced) than in the WT. In plants lacking PSI-G, the electrons are transferred faster on the donor side of PSI because of the higher affinity for Pc but the acceptor side apparently cannot accelerate the electron transfer and therefore electrons build up at the terminal acceptors of PSI.

3.5. In vitro stability of PSI in the thylakoids in light

As indicated from the measurements of redox state of the plastoquinone pool and from the photoinhibition experiments, PSI could be less stable in the absence of

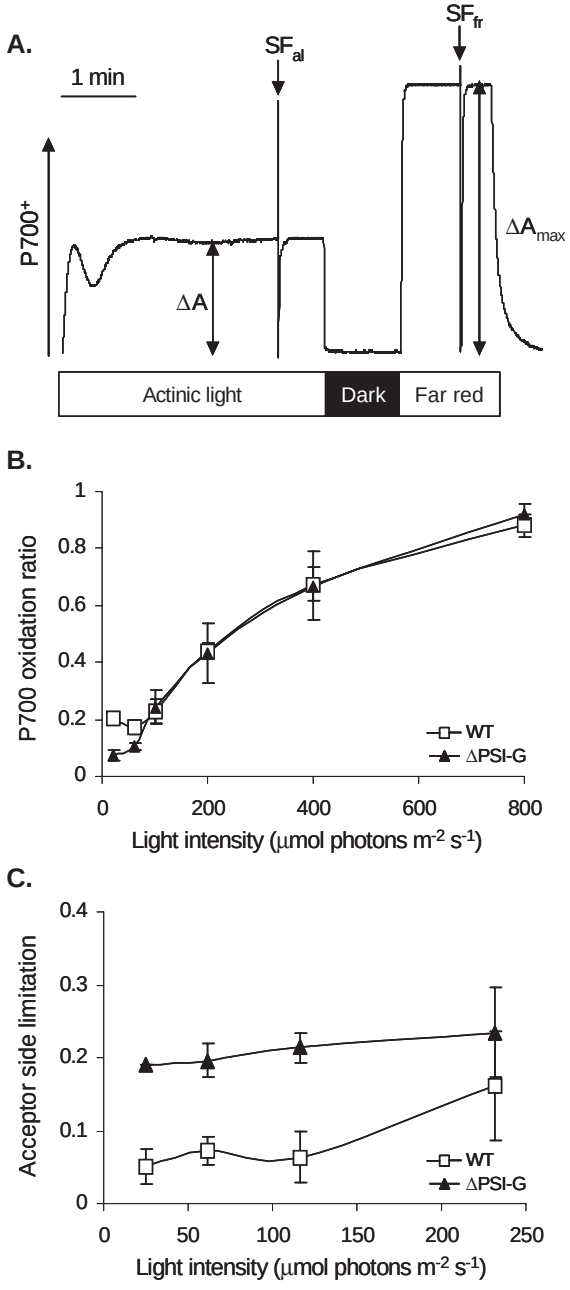

Fig. 4. P700 oxidation state in WT and ΔPSI-G leaves. (A) Method used to determine P700 oxidation ratio in vivo. A measurement of absorbance changes at 830 nm are shown in a WT leaf. The leaf was illuminated with actinic light with different light intensities (25–800 μmol photons m^{-2} s^{-1}) giving ΔA and far-red light to yield ΔAmax. Two 50 ms flashes of actinic light were applied during the actinic light (SF_{al}) and the far-red (SF_{fr}) illuminations. A trace using an intensity of 230 μmol photons m^{-2} s^{-1} actinic light is shown. The bars under the graph represent the periods of illumination with actinic light, darkness and far-red light, respectively. Total length of recording was 6 min. (B) Light-response of P700 oxidation ratio ($\Delta A/\Delta Amax$) in leaves of WT and ΔPSI-G. WT and knock-out PSI-G plants were used. (C) Light response of the acceptor side of PSI $(SF_{fr}-SF_{al})/SF_{fr}$ in leaves of WT and knock-out PSI-G. All data points in (B) and (C) represent the mean ± SD ($n=2$–3), but in some cases the error bars are covered by the marker.

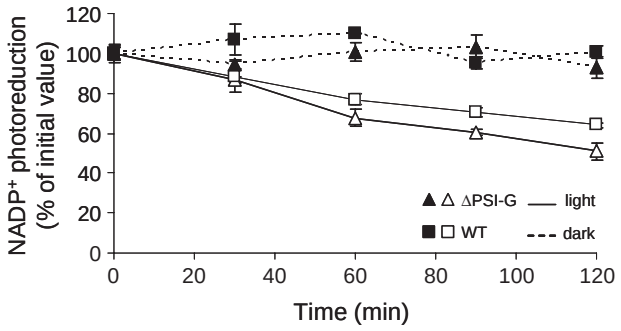

Fig. 5. Stability of PSI in WT and ΔPSI-G thylakoids in light. Thylakoid suspensions from WT and ΔPSI-G were illuminated with actinic light (150 μmol photons m^{-2} s^{-1}) and stirred in a thermostated chamber at 20 °C. A sample was removed every 30 min and the $NADP^+$ photoreduction activity was measured. Each point represents the relative $NADP^+$ photoreduction activity left ± SD (n=3); the low value of some of the error bars make them not visible. Initial activity was 51 μmol NADPH μmol^{-1} P700 s^{-1} for the WT and 71 μmol NADPH μmol^{-1} P700 s^{-1} for ΔPSI-G.

PSI-G. In order to address this directly, the stability of PSI in thylakoid membranes from both WT and plants devoid of PSI-G was investigated. Thylakoids were incubated in a chamber with gentle stirring in both darkness and in light (150 μmol photons m^{-2} s^{-1}). Every 30 min, samples were removed and the $NADP^+$ photoreduction activity was measured. In the thylakoids devoid of PSI-G, the $NADP^+$ photoreduction activity was reduced by 49% after 2 h whereas the decrease was only 36% in the WT (Fig. 5). Thus, PSI is less stable in the absence of PSI-G indicating that PSI-G has a role in the stability of the PSI complex during illumination.

4. Discussion

4.1. PSI-G is involved in the interaction between PSI and Pc

The binding dynamics study allowed us to estimate most of the kinetic constants in the reaction between Pc and P700 in *Arabidopsis*. The fast component represents the intra-complex transfer between Pc and P700, k_{et}, and it was measured to be 10 μs, which is in accordance with previous estimates [26]. In the absence of PSI-G, Pc has a higher affinity for P700 due to a difference in the dissociation characterized by k_{off}, meaning that Pc sits longer in the docking site of PSI. This difference in affinity for Pc in plants devoid of PSI-G explains a part—but not all—of the higher $NADP^+$ photoreduction activity previously reported [8]. According to the structural model of pea PSI, no part of PSI-G would seem to be close to the Pc docking site [4]. However, the 4.4 Å structural model does not reveal the docking site of Pc nor does it reveal the location of PSI-N [4]. It has been shown that the PSI-N subunit of PSI [9] and the PSI-F subunit [11,27] are involved in the interaction between PSI and Pc. In *Chlamydomonas reinhardtii*, four positive charges of the PSI-F subunit form the recognition site by electrostatic interactions with Pc [28], while tryptophane residues of the PSI-B and PSI-A subunits are also involved in the binding of Pc [29,30]. The interaction between PSI-G and Pc could possibly be via common interaction with another subunit, perhaps PSI-N, which is located at the PSI lumen. Thus, in *C. reinhardtii* removal of PSI-J, which is located away from the Pc docking site, results in less efficient Pc oxidation due to interactions via PSI-F [31].

The effect of PSI-G on Pc oxidation may be indirect, but it should be noted that removal of other peripheral subunits like PSI-K or PSI-O does not affect $NADP^+$ photoreduction activity [6,32]. The amino acid sequence of PSI-K is 30% identical to PSI-G and the two subunits are located at similar positions on the PSI-A and -B core subunits [4]. However, we cannot rule out that the absence of PSI-G may cause a conformational change in PSI-B that in turn affects Pc binding.

At high light intensities the different affinity for Pc does not affect redox conditions around PSI. However, at light intensities below 100 μmol photons m^{-2} s^{-1} the plants devoid of PSI-G oxidize Pc faster on the donor side of PSI leading to more reduced P700. In the WT about 20% of PSI is oxidized even at very low light conditions. It should be stressed that an almost identical light response for P700 oxidation has been reported by others [33,34]. At first sight the donor limitation might seem a disadvantage since at least 20% of PSI is essentially inactive even at low light conditions when a high quantum yield for PSI photochemistry would seem to be most important. However, the plants lacking PSI-G do not benefit from the more efficient donor side because they are limited by the acceptor side, which does not transfer the electrons faster to ferredoxin and subsequent acceptors. Hence, a comparable 20% of PSI complexes are inactive in the plants devoid of PSI-G, only now the limitation is at the acceptor side. Recent studies of mutants in cyclic electron transport have shown that preventing overreduction of the stroma by regulating the flow of electrons to PSI is essential for plants [33,34]. Apparently, PSI-G plays a role in this fine-tuning of PSI and contributes to regulating the supply of electrons to PSI at the donor side. The significance of this may be that reduced PSI acceptors are a source of reactive oxygen species, which may cause damage to PSI and other proteins and lipids in the chloroplast. In contrast, limiting PSI at the donor side not only prevents generation of reactive oxygen at the acceptor side of PSI but also leads to accumulation of $P700^+$, which is a good quencher of excited chlorophyll and thereby can prevent the production of singlet oxygen.

4.2. In the absence of PSI-G the PSI complex is less stable

Plants lacking the PSI-G subunit have 40% less PSI [8]. Despite the higher affinity of Pc for P700 and a higher in vitro $NADP^+$ photoreduction activity in the

absence of PSI-G, plants devoid of PSI-G cannot efficiently transport the electrons from PSII, and this results in a more reduced plastoquinone pool. The small increase in photodamage of PSII is most likely directly caused by the more reduced plastoquinone pool. PSI is much more damaged in the absence of PSI-G. However, the function of PSI-G in conveying PSI stability is clearly related to illumination whereas no difference in stability was seen in the dark. This could indicate that the role of PSI-G in stability and preventing photodamage is related to the regulation of the P700 redox state as explained above. Alternatively, the role of PSI-G in photoprotection of PSI is more direct and could for example be related to a protective role of the carotenoid molecule bound to PSI-G [35]. At present we cannot decide between these two possibilities.

Despite having 40% reduction of PSI, plants with no PSI-G protein have been reported to be indistinguishable from the WT under growth chamber conditions [8] but to show a decrease of about 20% in mean size when grown under greenhouse conditions [7]. The redox state of P700 differs in plants devoid of PSI-G compared to the WT at low light intensity (<100 μmol photons m^{-2} s^{-1}). Although this may be a disadvantage under most conditions, we have hypothesized that at very low light intensity the improved P700 reduction could be an advantage. However, preliminary results from growing plants lacking PSI-G and WT at very low light intensity (20 μmol photons m^{-2} s^{-1}) suggest that plants without PSI-G grow more slowly also under these conditions (data not shown).

Acknowledgments

This work was supported by The Danish National Research Foundation and by the EU (Contract No. HPRN-CT-2002-00248). The authors are grateful to Prof. Birger Lindberg Møller for invaluable discussions and support.

References

[1] P.E. Jensen, A. Haldrup, L. Rosgaard, H.V. Scheller, Molecular dissection of photosystem I in higher plants: topology, structure and function, Physiol. Plant. 119 (2003) 313–321.
[2] P. Jordan, P. Fromme, H.T. Witt, O. Klukas, W. Saenger, N. Krauss, Three-dimensional structure of cyanobacterial photosystem I at 2.5 Å resolution, Nature 411 (2001) 909–917.
[3] H.V. Scheller, P.E. Jensen, A. Haldrup, C. Lunde, J. Knoetzel, Role of subunits in eukaryotic photosystem I, Biochim. Biophys. Acta 1507 (2001) 41–60.
[4] A. Ben-Shem, F. Frolow, N. Nelson, Crystal structure of plant photosystem I, Nature 246 (2003) 630–635.
[5] S. Jansson, B. Andersen, H.V. Scheller, Nearest-neighbor analysis of higher-plant photosystem I holocomplex, Plant Physiol. 112 (1996) 409–420.
[6] P.E. Jensen, M. Gilpin, J. Knoetzel, H.V. Scheller, The PSI-K subunit of photosystem I is involved in the interaction between light-harvesting complex I and the photosystem I reaction center core, J. Biol. Chem. 275 (2000) 24701–24708.
[7] C. Varotto, P. Pesaresi, P. Jahns, A. Leβnick, M. Tizzano, F. Schiavon, F. Salamini, D. Leister, Single and double knockouts of the genes for photosystem I subunits G, K, and H of *Arabidopsis*, effects on photosystem I composition, photosynthetic electron flow, and state transitions, Plant Physiol. 129 (2002) 616–624.
[8] P.E. Jensen, L. Rosgaard, J. Knoetzel, H.V. Scheller, Photosystem I activity is increased in the absence of the PSI-G subunit, J. Biol. Chem. 277 (2002) 2798–2803.
[9] A. Haldrup, H. Naver, H.V. Scheller, The interaction between plastocyanin and photosystem I is inefficient in transgenic *Arabidopsis* plants lacking the PSI-N subunit of photosystem I, Plant J. 17 (1999) 689–698.
[10] J. Farah, F. Rappaport, Y. Choquet, P. Joliot, J.D. Rochaix, Isolation of a psaF-deficient mutant of *Chlamydomonas reinhardtii*: efficient interaction of plastocyanin with the photosystem I reaction center is mediated by the PsaF subunit, EMBO J. 14 (1995) 976–4964.
[11] A. Haldrup, D.J. Simpson, H.V. Scheller, Down-regulation of the PSI-F subunit of photosystem I (PSI) in *Arabidopsis thaliana*. The PSI-F subunit is essential for photoautotrophic growth and contributes to antenna function, J. Biol. Chem. 275 (2000) 31211–31218.
[12] S. Zhang, H.V. Scheller, Photoinhibition of PSI at chilling temperature and subsequent recovery in *Arabidopsis thaliana*, Plant Cell Physiol. 45 (2004) 1595–1602.
[13] S.E. Tjus, B.L. Møller, H.V. Scheller, Photosystem I is an early target of photoinhibition in barley illuminated at chilling temperatures, Plant Physiol. 116 (1998) 755–764.
[14] H.K. Lichtenhaler, Chlorophylls and carotenoids: pigments of photosynthetic biomembranes, Methods Enzymol. 148 (1987) 350–382.
[15] L.E. Ellefson, E.A. Ulrich, D.W. Krogmann, Plastocyanin, Methods Enzymol. 69 (1980) 223–228.
[16] H. Naver, M.P. Scott, J.H. Golbeck, B.L. Møller, H.V. Scheller, Reconstitution of barley photosystem I with modified PSI-C allows identification of domains interacting with PSI-D and PSI-A/B, J. Biol. Chem. 271 (1996) 8996–9001.
[17] F. Drepper, M. Hippler, W. Nitschke, W. Haehnel, Binding dynamics and electron transfer between plastocyanin and photosystem I, Biochemistry 35 (1996) 1282–1295.
[18] C. Klughammer, U. Schreiber, An improved method, using saturating light pulses, for the determination of photosystem I quantum yield via $P700^{+}$-absorbance changes at 830 nm, Planta 192 (1994) 261–268.
[19] C. Klughammer, U. Schreiber, Measuring P700 absorbance changes in the near infrared spectral region with a dual wavelength pulse modulation system, in: G. Garab (Ed.), Photosynthesis: Mechanisms and Effects, vol. V, Kluwer Academic Publishers, Dordrecht, 1998, pp. 4357–4360.
[20] H. Bottin, P. Mathis, Interaction of plastocyanin with the photosystem I reaction center: a kinetic study by flash absorption spectroscopy, Biochemistry 24 (1985) 6453–6460.
[21] M. Nordling, K. Sigfridsson, S. Young, L.G. Lundberg, Ö. Hansson, Flash-photolysis studies of the electron transfer from genetically modified spinach plastocyanin to photosystem I, FEBS Lett. 291 (1991) 327–330.
[22] K. Sigfridsson, S. Young, Ö. Hansson, Structural dynamics in the plastocyanin–photosystem 1 electron-transfer complex as revealed by mutant studies, Biochemistry 35 (1996) 1249–1257.
[23] J. Whitmarsh, Mobile electron carriers in thylakoids, in: L.A. Staehelin, C.J. Arntzen (Eds.), Photosynthesis III: Photosynthetic Membranes and Light Harvesting Systems, Encyclopedia of Plant Physiology, vol. 19, Springer-Verlag, Berlin, 1986, pp. 508–527.
[24] K. Sonoike, I. Terashima, Mechanism of photosystem I photoinhibition in leaves of *Cucumis sativus* l, Planta 194 (1994) 287–293.

[25] I. Terashima, S. Funayame, K. Sonoike, The site of photoinhibition in leaves of *Cucumis sativus* l. at low temperatures is photosystem I, not photosystem II, Planta 193 (1994) 300–306.
[26] E. Danielsen, H.V. Scheller, R. Bauer, L. Hemmingsen, M.J. Bjerrum, Ö. Hansson, Plastocyanin binding to photosystem I as a function of the charge state of the metal ion: effect of metal site conformation, Biochemistry 38 (1999) 11531–11540.
[27] M. Hippler, F. Drepper, W. Haehnel, J.D. Rochaix, The N-terminal domain of PsaF: precise recognition site for binding and fast electron transfer from cytochrome c6 and plastocyanin to photosystem I of *Chlamydomonas reinhardtii*, Proc. Natl. Acad. Sci. U. S. A. 95 (1998) 7339–7344.
[28] M. Hippler, J. Reichert, M. Sutter, E. Zak, L. Altschmied, U. Schroer, R.G. Herrmann, W. Haehnel, The plastocyanin binding domain of photosystem I, EMBO J. 15 (1996) 6374–6384.
[29] F. Sommer, F. Drepper, M. Hippler, The luminal helix l of PsaB is essential for recognition of plastocyanin or cytochrome c6 and fast electron transfer to photosystem I in *Chlamydomonas reinhardtii*, J. Biol. Chem. 277 (2002) 6573–6581.
[30] F. Sommer, F. Drepper, W. Haehnel, M. Hippler, The hydrophobic recognition site formed by residues PsaA-Trp651 and PsaB-Trp627 of photosystem I in *Chlamydomonas reinhardtii* confers distinct selectivity for binding of plastocyanin and cytochrome c6, J. Biol. Chem. 279 (2004) 20009–20017.
[31] N. Fischer, E. Boudreau, M. Hippler, F. Drepper, W. Haehnel, J.D. Rochaix, A large fraction of PsaF is nonfunctional in photosystem I complexes lacking the PsaJ subunit, Biochemistry 38 (1999) 5546–5552.
[32] P.E. Jensen, A. Haldrup, S. Zhang, H.V. Scheller, The PSI-O subunit of plant photosystem I is involved in balancing the excitation pressure between the two photosystems, J. Biol. Chem. 279 (2004) 24212–24217.
[33] Y. Munekage, M. Hashimoto, C. Miyake, K.I. Tomizawa, T. Endo, T. Masao, T. Shikanai, Cyclic electron flow around photosystem I is essential for photosynthesis, Nature 429 (2004) 579–582.
[34] Y. Munekage, M. Hojo, J. Meurer, T. Endo, M. Tasaka, T. Shikanai, PGR5 is involved in cyclic electron flow around photosystem I and is essential for photoprotection in *Arabidopsis*, Cell 110 (2002) 361–371.
[35] J.A. Ihalainen, P.E. Jensen, A. Haldrup, I.H. van Stokkum, R. van Grondelle, H.V. Scheller, J.P. Dekker, Pigment organization and energy transfer dynamics in isolated photosystem I (PSI) complexes from *Arabidopsis thaliana* depleted of the PSI-G, PSI-K, PSI-L, or PSI-N subunit, Biophys. J. 83 (2002) 2190–2201.